JOURNAL OF THEORETICAL AND APPLIED MECHANICS
61, 3, pp. 521-531, Warsaw 2023
https://doi.org/10.15632/jtam-pl/166652

AN UNSTEADY VEHICLE-ROAD COUPLING DYNAMIC RESPONSE OF A MULTI-LAYER PLATE ON A VISCOELASTIC HALF-SPACE FOUNDATION

Shao-Qi Li
Shijiazhuang Tiedao University, School of Transportation, Shijiazhuang, China
e-mail: llishaoqi@163.com
Zhan-You Yan
Shijiazhuang Tiedao University, State Key Laboratory of Mechanical Behavior in Traffic Engineering Structure and System Safety, Shijiazhuang, China, and
Shijiazhuang Tiedao University, School of Civil Engineering, Shijiazhuang, China
corresponding author, e-mail: yanzhanyou@163.com
Yong-Chang Cui, Xue-Ke Hou, Zi-Jun Wang
Shijiazhuang Tiedao University, School of Transportation and School of Civil Engineering, Shijiazhuang, China
e-mail: 749018248@qq.com, 2294232910@qq.com, 1151699829@qq.com

To study the dynamic response of roads under non-stationary random excitation, a dynamic differential equation is constructed firstly based on a two-axle half car model, and white noise to simulate road roughness is then filtered. Finally, non-stationary responses of different vehicle acceleration conditions are obtained. An infinite multi-layer plate on a viscoelastic half-space foundation as a model of the road structure and an analytical solution for the road dynamic response are obtained. Based on a numerical example, the dynamic response of a four-layer road model under vehicle loads is discussed. The study fills the gap in the theory of multi-wheel vehicle models.

Keywords: non-stationary filtered white noise, viscoelastic half-space, multi-layer plate, vehicle-road coupling

1. Introduction

With the continuous improvement of the national economic level and the rapid development of the road transportation industry, the number and types of various heavy-duty vehicles on the road are increasing, and damage to the road is particularly serious. Among them, vibration is an unavoidable topic when vehicles are driving on the road. Due to technical levels and other uncontrollable factors, the road surface cannot be completely flat because it leads to excitation of the road surface during driving of the vehicle. The vehicle vibration and its own gravity influence also produce complex dynamic response problems on the road surface (Rahman and Kibria, 2014; Awal *et al.*, 2017). How to establish a more realistic and effective model to reflect the dynamic response of the road under heavy loads has become a hot topic in the current road research.

At present, the dynamic response of the pavement under an external load is generally selected for a constant speed, and the upper load is described as a dead load or harmonic load. For the pavement structure model, early scholars usually simplified it to a Kirchhoff's thin plate on a viscoelastic foundation. Dieterman and Metrikine (1997) studied the dynamic response of single-layer soil under the action of a moving load as a simple harmonic load. Kim and Roesset (1998) and Kim (2004) studied the dynamic response of the infinite Kirchhoff thin plate on

the Kelvin foundation under a moving dead load and harmonic load by using the fast Fourier transform method. Sun (2007) used the integral transformation and Green function method to find the integral analytical solution of the transient deflection and the steady-state deflection of the plate under the moving load. Later, Cai *et al.* (2009) and Cao and Boström (2013) extended the road structure to an elastic half-space and porous saturated soil half-space volume models on the basis of Sun (2007). Li (2011) and Li *et al.* (2013) optimized the pavement structure model again: the infinite two-layer plate model on the viscoelastic half-space foundation was proposed, and the dynamic response of the two-layer plate structure under the moving load was studied. A relationship between the dynamic response of the plate structure and the elastic modulus of the material was obtained. Si (2017) extended the virtual excitation method to deal with random vibration of the viscoelastic half-space foundation under a train load, and used the evolutionary power spectrum and corresponding standard deviation to express time-varying random characteristics of the system. Mirsaidov and Mamasoliev (2020) established a mathematical model and a calculation method of the internal force coefficient of a multi-layer strip plate on an elastic foundation under various static loads and proved regularity of infinite algebraic equations and obtained the corresponding estimation. Hamidi *et al.* (2021) utilized the state space method in the Laplace domain. The influence of the elastic foundation and viscoelastic interface on dynamic behavior of laminated magneto electro elastic rectangular plates with simply supported boundary conditions was studied. The dynamic response of three--dimensional displacement, stress, electric displacement and magnetic displacement phase in the thickness direction and orthotropic behavior under harmonic stress was analyzed. However, the current speed of vehicles on the road is always changing, especially acceleration and deceleration when the vehicle starts and stops, which result in that the load on the road can not be simply described as a dead or harmonic loads.

The article combines the vehicle load with random road roughness excitation for the first time. The authors use a two-axle and half-car model to build dynamic differential equations, and used filtered white noise to simulate road roughness. At the same time, the viscoelastic half--space foundation model is further extended to a multi-layer plate on a viscoelastic half-space foundation model. Based on Green's function and Duhamel's integral, the analytical solution of the dynamic response of the infinite multi-layer plate on the viscoelastic half-space foundation under the action of moving vehicles is obtained, and the generalized integral calculation program for simulating singular and oscillating functions is compiled by using MATLAB software. Finally, the algorithm in this paper is created and the dynamic response of the road structure under non-stationary vehicle-road coupling conditions is obtained.

2. Vehicle and road model

2.1. Vehicle model

The vehicle model is a two-axle heavy vehicle, and the half-car model is shown in Fig. 1a. The tire damping is relatively small compared to suspension damping, and for convenience of numerical calculations, the vehicle model can be simplified as shown in Fig. 1b.

Based on the balance of the front and rear forces of the vehicle body, it is concluded that

$$\begin{aligned} &m_{2f}\ddot{z}_{2f} + m_{2c}\ddot{z}_c\frac{b}{L} + C_{2f}(\dot{z}_{2f} - \dot{z}_{1f}) + K_{2f}(z_{2f} - z_{1f}) = 0 \\ &m_{2r}\ddot{z}_{2r} + m_{2c}\ddot{z}_c\frac{a}{L} + C_{2r}(\dot{z}_{2r} - \dot{z}_{1r}) + K_{2r}(z_{2r} - z_{1r}) = 0 \end{aligned} \tag{2.1}$$

Adding Eqs. (2.1), we get

$$m_2\ddot{z}_c + C_{2f}(\dot{z}_{2f} - \dot{z}_{1f}) + C_{2r}(\dot{z}_{2r} - \dot{z}_{1r}) + K_{2f}(z_{2f} - z_{1f}) + K_{2r}(z_{1r} - z_{2r}) = 0 \tag{2.2}$$

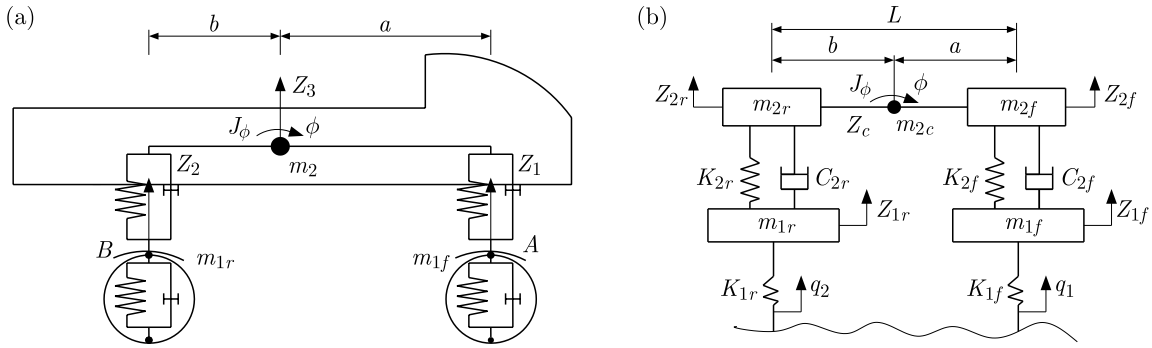

Fig. 1. Vehicle model: (a) two-axle half-car model, (b) simplified half-car model

Based on the balance of the front and rear forces of the non-suspended mass, it is concluded that

$$\begin{aligned} &m_{1f}\ddot{z}_{1f} + C_{2f}(\dot{z}_{1f} - \dot{z}_{2f}) + K_{2f}(z_{1f} - z_{2f}) + K_{1f}(z_{1f} - q_1) = 0 \\ &m_{1r}\ddot{z}_{1r} + C_{2r}(\dot{z}_{1r} - \dot{z}_{2r}) + K_{2r}(z_{1r} - z_{2r}) + K_{1r}(z_{1r} - q_2) = 0 \end{aligned} \tag{2.3}$$

Based on the principle of moment balance around the centroid, it is concluded that

$$J\ddot{\phi} - aC_{2f}(\dot{z}_{2f} - \dot{z}_{1f}) + bC_{2r}(\dot{z}_{2r} - \dot{z}_{1r}) - aK_{2f}(z_{2f} - z_{1f}) + bK_{2r}(z_{2r} - z_{1r}) = 0 \tag{2.4}$$

According to the literature (Zhang *et al.*, 2022), the road roughness of the front and rear wheels in the time domain is expressed as

$$\dot{q}_f(t) + \dot{s}2\pi n_c q(t) = 2\pi n_0 \sqrt{G_q(n_0)\dot{s}}W(t) \qquad \dot{q}_r(t) = -\frac{2v}{L}q_r(t) - \dot{q}_f(t) + \frac{2v}{L}q_f(t) \tag{2.5}$$

where $q(t)$ is the road roughness under unsteady conditions in the time domain, s is the distance traveled by the vehicle, n_c is the lower cut-off space frequency, $n_c = 0.011\,\mathrm{m}^{-1}$, $n_0 = 0.1\,\mathrm{m}^{-1}$ is the reference space frequency, $G_q(n_0)$ is the road roughness coefficient – if it is not stated in the text, it is taken as Class C pavement (ISO, 1990), $W(t)$ is the band-limited white noise, v is the vehicle running speed, L is the distance between the front and rear wheels.

2.2. A multi-layer plate on the viscoelastic half-space foundation

Figure 2 shows an infinite multi-layer plate model on a viscoelastic half-space foundation. The bottom layer shown in the figure is a viscoelastic half-space foundation and above it, is an infinite multi-layer plate.

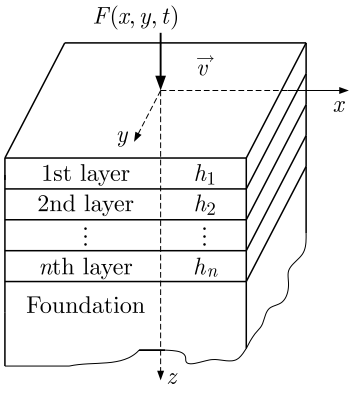

Fig. 2. An infinite multi-layer plate on a viscoelastic half-space foundation

The density, Poisson's ratio and elastic modulus of the viscoelastic half-space foundation are represented by ρ, μ and E, respectively. The displacement in three directions of x, y, z is represented by $u_i(u_x, v_y, w_z)$, and the control equation for a homogeneous isotropic viscoelastic half-space foundation represented by the displacement is

$$(\lambda + G)\nabla(\nabla \cdot u_j) + G\nabla^2 u_j = \rho \frac{\partial^2 u_j}{\partial t^2} \tag{2.6}$$

where: λ, G are Lamé constants, $\lambda = \mu E/[(1+\mu)(1-2\mu)]$, $G = E/[2(1+\mu)]$, ∇^2 is the Laplace operator.

However, in practice, soil (i.e. viscoelastic half-space) should also consider the influence of material damping. According to the linear hysteresis damping theory, material damping is introduced, namely

$$E^* = (1 + 2\mathrm{j}\xi)E \qquad G^* = (1 + 2\mathrm{j}\xi)G \qquad \lambda^* = (1 + 2\mathrm{j}\xi)\lambda \tag{2.7}$$

where j is the imaginary unit, $\mathrm{j}^2 = -1$, ξ is the material damping ratio, where $\xi = 0.05$ is taken.

Smooth contact between the plate and the viscoelastic half-space foundation is assumed. The thickness, elastic modulus, Poisson's ratio and density of each layer are h_i, E_i, μ_i, ρ_i $(i = 1, 2, 3)$. The upper surface of the uppermost plate is subjected to a moving load of $F(x, y, t)$. $P(x, y, t)$ is the vertical reaction of the viscoelastic half-space foundation acting on the plate. In reference (Yang *et al.*, 2010), the differential equation of motion expressed by the vertical displacement of the multi-layer plate is

$$D\Big(\frac{\partial^4 w_{zb}}{\partial x^4} + \frac{\partial^4 w_{zb}}{\partial y^4}\Big) + 2(D_{xy} + 2D_k)\frac{\partial^4 w_{zb}}{\partial x^2 \partial y^2} + m_b \frac{\partial^2 w_{zb}}{\partial t^2} = F(x, y, t) - P(x, y, t) \tag{2.8}$$

where w_{zb} is vertical displacement of the multi-layer plate, $m_b = \sum_{i=1}^{n} \rho_i h_i$ is mass per unit area of the multi-layer plate, D is bending stiffness of the plate in either the x or y direction, D_{xy} is bending stiffness in both the x and y directions, D_k is torsional stiffness. Its expression is

$$\begin{aligned}
D &= \int_{h_0-h_1}^{h_0} \frac{E_1}{1-\mu_1^2} z^2\, dz + \int_{h_0-h_1-h_2}^{h_0-h_1} \frac{E_2}{1-\mu_2^2} z^2\, dz + \cdots + \int_{h_0-\sum_{i=1}^{n} h_i}^{h_0-\sum_{i=1}^{n-1} h_i} \frac{E_n}{1-\mu_n^2} z^2\, dz \\
D_{xy} &= \int_{h_0-h_1}^{h_0} \frac{E_1\mu_1}{1-\mu_1^2} z^2\, dz + \int_{h_0-h_1-h_2}^{h_0-h_1} \frac{E_2\mu_2}{1-\mu_2^2} z^2\, dz + \cdots + \int_{h_0-\sum_{i=1}^{n} h_i}^{h_0-\sum_{i=1}^{n-1} h_i} \frac{E_n\mu_n}{1-\mu_n^2} z^2\, dz \\
D_k &= \int_{h_0-h_1}^{h_0} \frac{E_1}{2(1+\mu_1)} z^2\, dz + \int_{h_0-h_1-h_2}^{h_0-h_1} \frac{E_2}{2(1+\mu_2)} z^2\, dz + \cdots + \int_{h_0-\sum_{i=1}^{n} h_i}^{h_0-\sum_{i=1}^{n-1} h_i} \frac{E_n}{2(1+\mu_n)} z^2\, dz
\end{aligned} \tag{2.9}$$

where h_0 is the distance between the neutral layer of the multi-layer plate and the upper surface of the uppermost plate. Since the stress in the neutral layer is zero (Hung and Yang, 2001), the expression can be deduced as follows

$$h_0 = \left[E_1 h_1^2 + E_2(2h_1 + h_2)h_1 + E_3(2h_1 + 2h_2 + h_3)h_3 + \cdots + E_n\left(2\sum_{i=1}^{n-1} h_i + h_n\right)h_n\right] \frac{1}{n\sum_{i=1}^{n} E_i h_i} \tag{2.10}$$

The boundary conditions and initial conditions of the problem can be expressed as

$$\begin{aligned}
&\lim_{x\to\pm\infty} \frac{\partial^n w_{zb}}{\partial x^n} = 0 \qquad \lim_{y\to\pm\infty} \frac{\partial^n w_{zb}}{\partial y^n} = 0 \qquad n = 0, 1, 2, \ldots \\
&w_{zb}(x, y, t)\big|_{t=0} = \frac{\partial w_{zb}(x, y, t)}{\partial t}\Big|_{t=0} = 0
\end{aligned} \tag{2.11}$$

2.3. Description of the vehicle-road coupling system

The article studies the dynamic response of road structures based on the vehicle-road coupling. The coupling relationship between the vehicle and the road surface can be described as follows: when the vehicle passes through the road at a certain speed, the vehicle generates vibration due to excitation of the road roughness, and the road structure also vibrates under the dynamic load of the vehicle, and the vibration of the road surface causes secondary coupling vibration of the vehicle.

In order to more accurately describe the interaction between the tire and road surface, the vertical load force $F(x,y,t)$ consists of two parts, namely the static load Mg (M is mass distributed on the tire by the whole vehicle) and the dynamic load F_d (Lu *et al.*, 2021)

$$F = Mg + F_d \tag{2.12}$$

where F_d is the reaction force generated by the unsteady road excitation on the vehicle.

3. Analytical solution of the dynamic response

According to the Helmholtz theorem, the displacement vector of a viscoelastic half-space foundation in a rectangular coordinate system can be decomposed into

$$\mathbf{u}_i(u_x, v_y, w_z) = \nabla\Phi + \nabla \times \mathbf{\Psi}_i(\Psi_1, \Psi_2, \Psi_3) \tag{3.1}$$

where u_x, v_y and w_z are displacements in the three directions x, y and z of the viscoelastic half-space foundation, respectively, Φ is the scalar potential of displacement $\mathbf{u}_i$, $\mathbf{\Psi}_i$ is the vector potential of the displacement $\mathbf{u}_i$.

By using Green's function and generalized Duhamel's integral, an analytical solution of the dynamic response of an infinite four-layer plate on a viscoelastic half-space foundation under moving loads can be obtained. The expression for the generalized Duhamel integral is (Li *et al.*, 2013)

$$u_{ki}(x,y,z,t) = \int\limits_S \int\limits_0^t F(\zeta_1,\zeta_2,\tau) G_{ki}(x-\zeta_1, y-\zeta_2, z, t-\tau)\, d\tau\, dS \tag{3.2}$$

where on the right-hand there is a convolution integral of the moving load and Green's function.

According to reference (Li *et al.*, 2013), the vertical displacement of the viscoelastic half-space foundation under the moving load can be obtained

$$\begin{aligned} w = {} & \frac{F}{(2\pi)^2 G} \mathrm{e}^{\mathrm{j}\omega_0 t} \int\limits_{-\infty}^{+\infty}\int\limits_{-\infty}^{+\infty} \frac{\sin(k_1 l_1)}{k_1 l_1} \frac{\sin(k_2 l_2)}{k_2 l_2} \frac{1}{\Delta} [B_p(k_1^2 + k_1^2 + B_s^2)\mathrm{e}^{-B_p z} \\ & - 2B_p(k_1^2 + k_2^2)\mathrm{e}^{-B_s z}] \mathrm{e}^{\mathrm{j}[k_1(x-vt)+k_2 y]}\, dk_1\, dk_2 \end{aligned} \tag{3.3}$$

where ω_0 is the loading frequency of harmonic loads, $\omega_0 = 0$ represents the moving dead load, $l_1 = 0.11$, $l_2 = 0.16$ are the rectangular areas of contact force distribution between the wheel and ground. The rectangular area is $\{-l_1 \leqslant x \leqslant l_1,\ -l_2 \leqslant x \leqslant l_2\}$, and B_p, B_s, Δ are intermediate transition expressions. The derivation is more complex and will not be repeated, see Li *et al.* (2013). v is the driving speed of the vehicle, and the range of it is 0-45 m/s.

4. Numerical calculation

4.1. Vehicle and road model parameters

The analytical solution for the multi-layer plate on the viscoelastic half-space foundation has been given in Section 3. Next, the authors completed simulation of the dynamic response using MATLAB (Xue, 2019; Kreines and Kreines, 2020). In fact, the making use of four layer plates such as surface layer, base, subbase and cushion layer is sufficient to meet the needs of the project. That is, $n = 4$ in Eqs. (2.9) and (2.10). The article takes the road structure of Laiqu section of Taihang Mountain Expressway as the example (Yan *et al.*, 2020), see Table 1 for material parameters of the viscoelastic half-space foundation and the four-layer plate structure. The parameter information of the two-axle heavy vehicle is given in Table 2 (Kim *et al.*, 2005).

Table 1. Material parameters of the road structure

Pavement structure	Thickness [m]	Elastic modulus [MPa]	Poisson's ratio	Density [kg/m^3]
AC-13C	0.04	9000	0.25	2300
ARHM-20	0.06	10000	0.25	2300
ATB-25	0.1	8000	0.25	2400
Subbase	0.54	9000	0.25	2300
Foundation	$+\infty$	60	0.40	1850

Table 2. Parameters of the two-axle heavy vehicle

Parameter	Numerical value	Parameter	Numerical value
Front wheel mass [kg]	500	Rear suspension damping [Ns/m]	$3.3420 \cdot 10^7$
Rear wheels mass [kg]	725	Front suspension stiffness [N/m]	$1.577 \cdot 10^6$
Vehicle mass [kg]	28500	Rear suspension stiffness [N/m]	$4.724 \cdot 10^6$
Wheel base [m]	4	Front wheel stiffness [N/m]	$3.146 \cdot 10^6$
Front suspension damping [Ns/m]	$1.120 \cdot 10^7$	Rear wheels stiffness [N/m]	$4.724 \cdot 10^6$

4.2. Road surface excitation in an unsteady state

The roughness parameters corresponding to A-D grade roads refer to the current standard GB/T 7031-2005 (Li *et al.*, 2006), see Table 3. According to equations $(2.5)_2$ and (2.6), filtered white noise is used to simulate road roughness at the front and rear wheel positions.

Table 3. A-D pavement grade parameters in GB/T 7031-2005

Pavement grade	Unevenness parameter $G_d(n_0)$ $[10^{-6}(\mathrm{m}^2/\mathrm{m}^{-1})]$		
	minimum	geometric mean	maximum
A	–	16	32
B	32	64	128
C	128	256	512
D	512	1024	2048

Figure 3a shows the time history response of road roughness of different pavement grades in an unsteady state. The vehicle speed uniformly increases from 0 m/s to 45 m/s. Negative

values represent a situation below the road reference plane. At 12 seconds, the time history response of road roughness under four different pavement grades A, B, C and D based on band-limited white noise is 7.855 mm, 15.710 mm, 31.420 mm and 62.840 mm, respectively. They are all extreme values in 15 seconds. Except for A-level pavement, all of them are doubled on the basis of the previous grade. Taking the D-level pavement as an example, a small speed from 0 s to 2 s produces a small displacement response, and the response increases with an increase of speed. When the speed is greater than 7 m/s, its amplitude fluctuates within the range of 0 mm to 62.840 mm. Figure 3b shows the time history response of road roughness at the front tire and rear tire positions under non-stationary conditions. As shown in the figure, from 0 s to 15 s, the road roughness curves at the front and rear wheel positions appear successively, and the two curves gradually overlap as the vehicle speed increases. However, from 0 s to 2 s, the two curves differ from the above conclusion due to wheelbase length of the front and rear wheels. Figure 3c shows the road roughness with different accelerations. From the slopes of the two curves in the figure, it can be seen that the greater the acceleration, the stronger the increase (or decrease) in the amplitude of road roughness. This phenomenon conforms to Newton's second law which it states that the magnitude of the force acting (road roughness in the article) on an object is proportional to acceleration.

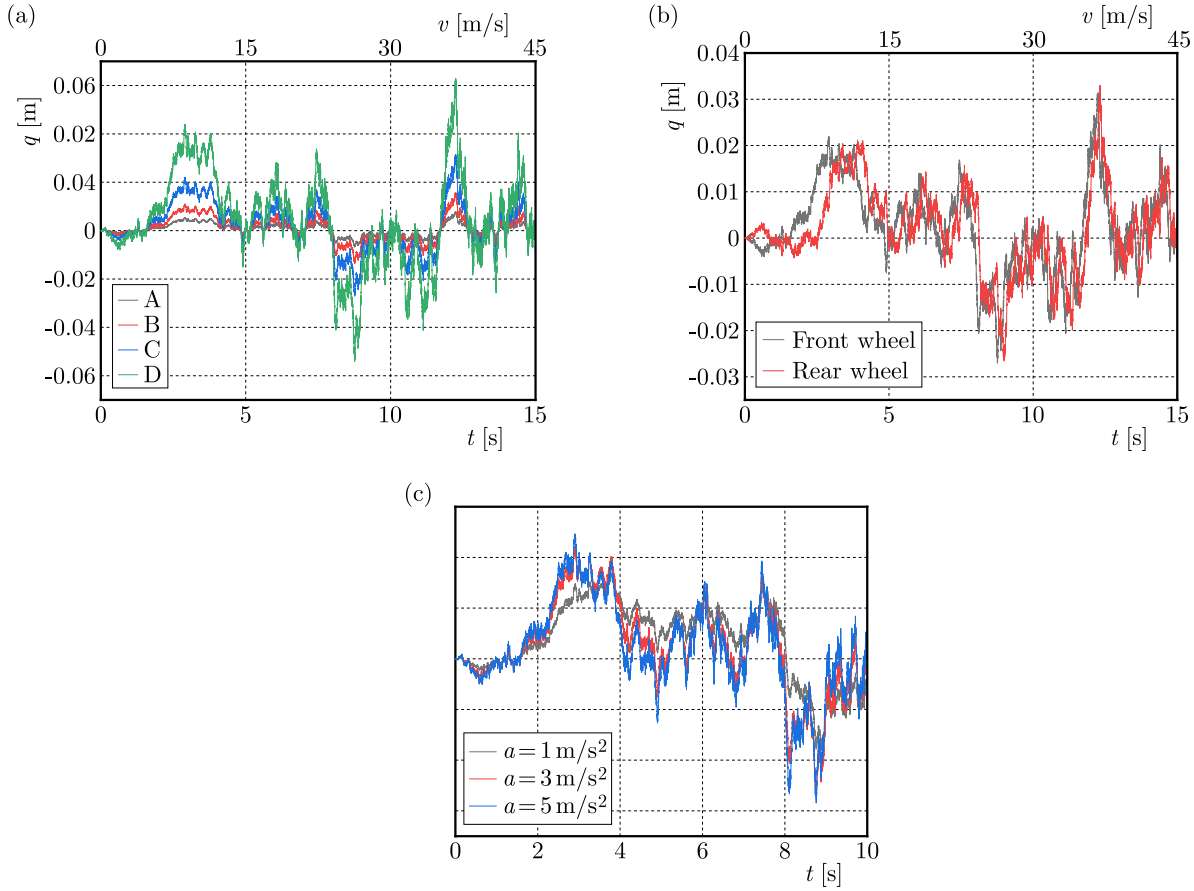

Fig. 3. Road roughness: (a) of different pavement grades, (b) under various tires, (c) with different accelerations

Figure 4a shows the vertical vibration time-history response of the unsprung mass of the front axle. Its amplitude fluctuates around the $w = 0$ axis and increases with an increase of the vehicle speed, which has a strong correlation with the road roughness response. According to equation (2.12), the C-level road excitation under the non-stationary vehicle load, as shown in Fig. 4b, can be obtained. Its amplitude fluctuates up and down around the static load generated

by the vehicle self weight ($Mg/4 = 7.5827 \cdot 10^7$ N), which shows an increasing trend as the vehicle speed increases. From 0 s to 15 s, the maximum and minimum values of the road excitation are $7.584 \cdot 10^7$ N and $7.581 \cdot 10^7$ N, respectively. The difference between them is only 0.04%. Its value directly affects the result of vertical displacement of the pavement.

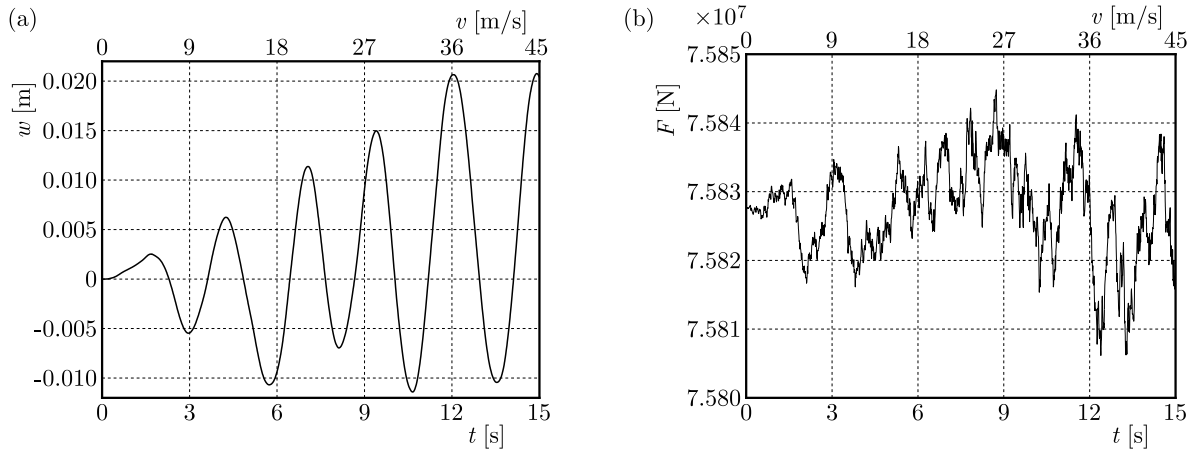

Fig. 4. (a) Unsprung mass vertical vibration of the front axle; (b) road excitation in an unsteady state

4.3. Dynamic response of the vehicle-road coupling in an unsteady state

4.3.1. Algorithm validation

Hung used the direct integral transformation method to calculate the dynamic response of a viscoelastic half-space foundation (Hung and Yang, 2001). Next, the article uses a self-made MATLAB program to study the dynamic response of road structures. Some model parameters in Hung's article are as follows: $v = 50$ km/h, $F = 5 \cdot 10^4$ N, $G = 20$ MPa, $\mu = 0.25$, $\rho = 2000$ kg/m^3, $\xi = 0.02$. To verify the correctness of the self-made MATLAB program, see Fig. 5, where a comparison of the time-history response results of the vertical displacement W of viscoelastic the half-space foundation is shown. The method in this paper is consistent with the calculation results of Hung. Li *et al.* (2015) established a layered road structure using Ansys software and verified the correctness of the algorithm proposed in this paper.

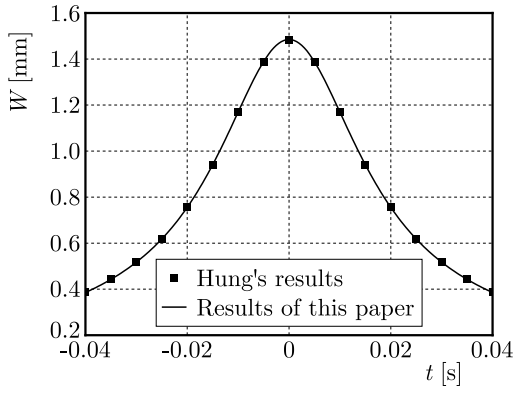

Fig. 5. Comparison of the vertical displacement results

4.3.2. Displacement response of the four-layer plate under an unsteady state

The force exerted by driving vehicles on the road surface can cause vertical displacement of the road surface. This Section focuses on the displacement w of a four-layer plate on a viscoelastic half-space foundation.

Figure 6a shows the time history curve of the vertical displacement of the road surface, four curves represent four different vehicle speeds. When the speed is 5 m/s, 10 m/s, 20 m/s, and 30 m/s, the vertical displacements are ±0.6 s are 0.131 mm, 0.057 mm, 0.027 mm, and 0.018 mm, respectively. Figure 6b shows the vertical displacement under a single wheel in the direction of x (driving direction) and y (perpendicular to the driving direction) when the moving speed is 10 m/s. At 6 m from the reference point, their vertical displacement is $5.677 \cdot 10^{-2}$ mm and $5.796 \cdot 10^{-2}$ mm, respectively, with a difference of only 2.096%. For the observation point, the vertical displacement gradually increases when the vehicle arrives, and decreases when the vehicle leaves. Generally, it presents a "V" shape with flat ends and steep middle. Figure 6c shows three curves representing the vertical displacement of the road surface at the front wheel position, where the rear wheel and the front wheel act alone, and the front and rear wheels act together ($v = 10$ m/s). The maximum vertical displacement of a single wheel is 0.094 mm, 0.340 mm respectively, and the maximum vertical displacement caused by the combined action of two wheels is 0.434 mm.

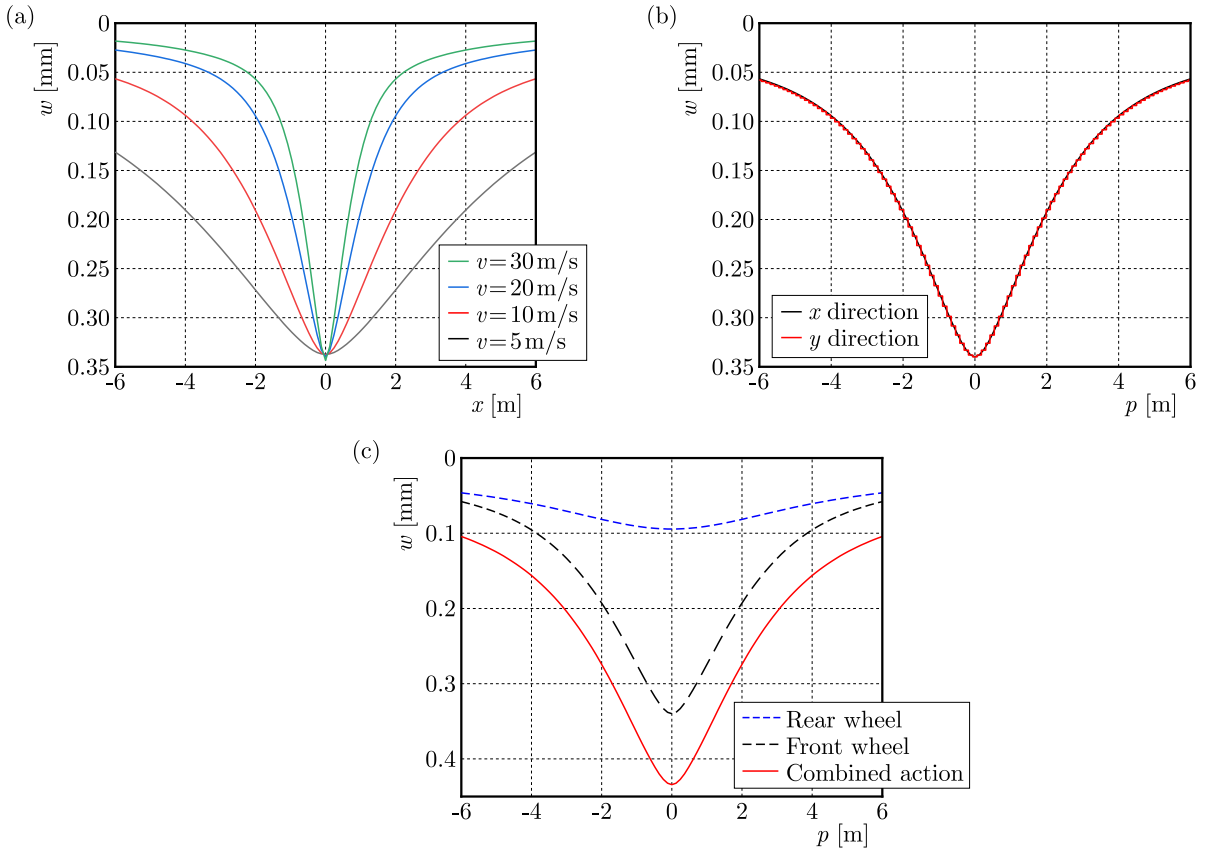

Fig. 6. (a) Time history curve of vertical displacement at different speeds; (b) vertical displacement in x and y directions; (c) vertical displacement of each tire at the front wheel position

Figure 7a shows the vertical displacement response nephogram of the four-layer plate caused by the single-wheel action. Figure 7b shows the interaction of the front and rear wheels ($v = 15$ m/s). The maximum vertical displacement is 0.340 mm, 0.438 mm, respectively. The combined action of the front and rear wheels is 1.288 times of a single wheel. The vertical displacement effect of a single wheel set on the pavement is shown as a "circle" extending from the inside out on a plane. During the double-wheel action, due to the two "circular" coherent effects, it gradually transits to "8-shaped" and "oval", and finally approaches to "circular" infinitely.

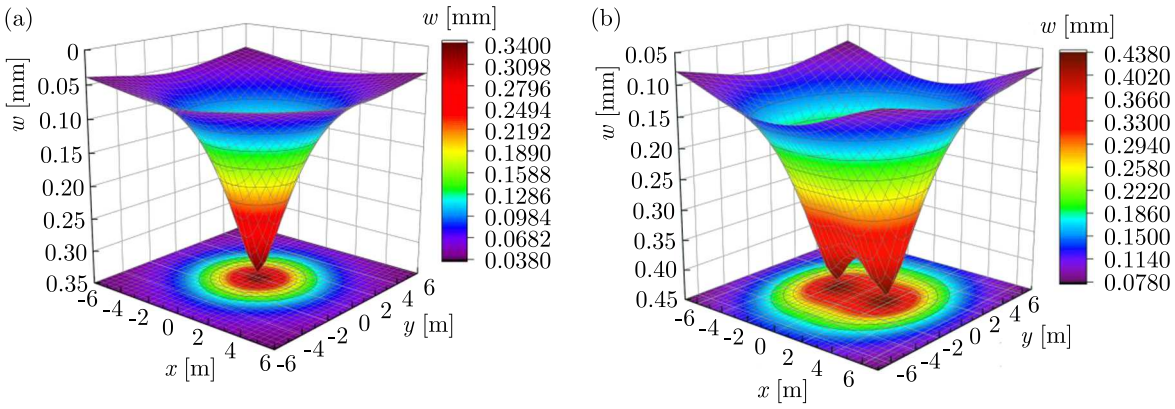

Fig. 7. Nephogram of vertical displacement: (a) under the action of a single wheel, (b) under the coherent action of the front and rear wheels

5. Conclusions

By establishing a mathematical model and rigorous theoretical derivation, the unsteady vehicle--road coupling dynamic response of a multi-layer plate on a viscoelastic half space foundation is studied, and the following conclusions are drawn:

- Based on band-limited white noise to simulate road roughness, the response of road roughness is small at a low speed, but increases significantly with speed. At high speeds, the response of road roughness is relatively large, but the increase in speed is relatively small, and there may even be a decrease.
- Based on the non-steady road excitation of accelerating vehicles, its amplitude fluctuates around the static load generated by the vehicle own weight, and increases with an increase of vehicle speed.
- The vertical displacement effect of the vehicle load on the ground is almost the same in the longitudinal direction (driving direction) and the transverse direction (perpendicular to the driving direction). The transverse displacement at 6m from the loading position is only 2.096% higher than the longitudinal displacement, and this effect decreases rapidly with an increase of distance.
- The vertical displacement effect of a single wheel set on the pavement is shown as a "circle" extending from the inside out on a plane. During the double-wheel action, due to the two "circular" coherent effects, it gradually transits to "8-shaped" and "oval", and finally approaches to "circular" infinitely.

References

1. Awal M.A., Ouelha S., Dong S., Boashash B., 2017, A robust high-resolution time-frequency representation based on the local optimization of the short-time fractional Fourier transform, *Digital Signal Processing*, **70**, 125-144

2. Cai Y.Q., Cao Z.G., Sun H.L., Xu C., 2009, Dynamic response of pavements on poroelastic half-space soil medium to a moving traffic load, *Computers and Geotechnics*, **36**, 52-60

3. Cao Z.G., Boström A., 2013, Dynamic response of a poroelastic half-space to accelerating or decelerating trains, *Journal of Sound and Vibration*, **332**, 2777-2794

4. Dieterman H.A., Metrikine A., 1997, Critical velocities of a harmonic load moving uniformly along an elastic layer, *Journal of Applied Mechanics – ASME*, **64**, 596-600

5. Hamidi M., Zaki S., Aboussaleh M., 2021, Modeling and numerical simulation of the dynamic behavior of magneto-electro-elastic multilayer plates based on a Winkler-Pasternak elastic foundation, *Journal of Intelligent Material Systems and Structures*, **32**, 832-846
6. Hung H.H., Yang Y.B., 2001, Elasitc waves in visco-elastic half-space generated by various vehicle loads, *Solid Dynamics and Earthquake Engineering*, **21**, 1-17
7. ISO 8606:1990 – Plastics – Prepregs – Bulk moulding compound (BMC) and dough moulding compound (DMC) – Basis for a specification
8. Kim C.W., Kawatani M., Kim K.B., 2005, Three-dimensional dynamic analysis for bridge-vehicle interaction with roadway roughness, *Computers and Structures*, **83**, 1627-1645
9. Kim S.M., 2004, Influence of horizontal resistance at plate bottom on vibration of plates on elastic foundation under moving loads, *Engineering Structures*, **26**, 519-529
10. Kim S.M., Roesset J.M., 1998, Moving loads on a plate on elastic foundation, *Journal of Engineering Mechanics*, **124**, 1010-1017
11. Kreines M.G., Kreines E.M., 2020, Matrix models of texts: models of text collections, *Mathematical Models and Computer Simulations*, **12**, 37-57
12. Li H.Y., 2011, *Research on Pavement Structure Dynamics under the Interaction between Vehicle and Pavement* (in Chinese), Beijing Jiaotong University
13. Li H.Y., Qi Y.Q., Liu J., 2013, Dynamic responses of a two-layer plate on viscoelastic half-space foundation under moving loads (in Chinese), *Geotechnical Mechanics*, **34**, 28-34
14. Li H.Y., Yang S.P., Liu J., Si C.D., 2015, Dynamic response in multilayered viscoelastic medium generated by moving distributed loads (in Chinese), *Engineering Mechanics*, **32**, 120-127
15. Li S.C., Wang S.Y., Zhao J.Y., 2006, Mechanical vibration road surface spectrum measurement data report: GB/T7031-2005 (in Chinese), Beijing: China Standards Press
16. Lu Y.J., Zhang J.N., Li H.Y., Ma Z.Z., 2021, Study on coupling dynamics of tire-road system based on non-uniform contact (in Chinese), *Journal of Mechanical Engineering*, **57**, 87-98
17. Mirsaidov M., Mamasoliev Q., 2020, Contact problems of multilayer slabs interaction on an elastic foundation, *IOP Conference Series: Earth and Environmental Science*, **614**, 1-14
18. Rahman M.S., Kibria K.M.G., 2014, Investigation of vibration and ride characteristics of a five degrees of freedom vehicle suspension system, *Procedia Engineering*, **90**, 96-102
19. Si L.T., 2017, *Random Vibration Analysis of Linear Continuous System under Moving Random Load* (in Chinese), Dalian University of Technology
20. Sun L., 2007, Steady-state dynamic response of a Kirchhoffs slab on viscoelastic Kelvin's foundation to moving harmonic loads (in Chinese), *Journal of Applied Mechanics*, **74**, 1212-1224
21. Xue D.Y., 2019, *MTALAB Calculus* (in Chinese), Beijing: Tsinghua University Press
22. Yan Z.Y., Zhao X.L., Zhao G.F., Zhao Y., Zhao G.Y., 2020, Dynamic response of asphalt pavement under multi-wheel dynamic load (in Chinese), *Journal of China Highway*, **33**, 119-132
23. Yang S.P., Li S.H., Lu Y.J., 2010, Investigation on dynamical interaction between a heavy vehicle and road pavement, *Vehicle System Dynamics: International Journal of Vehicle Mechanics and Mobility*, **48**, 923-944
24. Zhang B.Y., Dai T., Tan C.A., Li J., Zhang Y., Li S.H., 2022, Research on the non-stationary virtual excitation method of suspension system vibration characteristics (in Chinese), *Vibration. Test and Diagnosis*, **42**, 227-234

Manuscript received February 8, 2023; accepted for print May 16, 2023